Lab on a Chip

PAPER

View Article Online
View Journal | View Issue

Cite this: *Lab Chip*, 2021, **21**, 3899

Simultaneous measurement of contractile force and field potential of dynamically beating human iPS cell-derived cardiac cell sheet-tissue with flexible electronics†

Takashi Ohya,[ab] Haruki Ohtomo,[a] Tetsutaro Kikuchi,[c] Daisuke Sasaki,[c] Yohei Kawamura,[bd] Katsuhisa Matsuura,[c] Tatsuya Shimizu,[c] Kenjiro Fukuda, *[b] Takao Someya *[be] and Shinjiro Umezu *[a]

Received 10th May 2021,
Accepted 5th August 2021

DOI: 10.1039/d1lc00411e

rsc.li/loc

Human induced pluripotent stem (iPS) cell-derived cardiomyocytes are used for *in vitro* pharmacological and pathological studies worldwide. In particular, the functional assessment of cardiac tissues created from iPS cell-derived cardiomyocytes is expected to provide precise prediction of drug effects and thus streamline the process of drug development. However, the current format of electrophysiological and contractile assessment of cardiomyocytes on a rigid substrate is not appropriate for cardiac tissues that beat dynamically. Here, we show a novel simultaneous measurement system for contractile force and extracellular field potential of iPS cell-derived cardiac cell sheet-tissues using 500 nm-thick flexible electronic sheets. It was confirmed that the developed system is applicable for pharmacological studies and assessments of excitation–contraction coupling-related parameters, such as the electro-mechanical window. Our results indicate that flexible electronics with cardiac tissue engineering provide an advanced platform for drug development. This system will contribute to gaining new insight in pharmacological study of human cardiac function.

Introduction

The technology of producing cardiomyocytes from human pluripotent stem (PS) cells (embryonic stem [ES] cells, induced pluripotent stem [iPS] cells) has seen dramatic development in recent years.[1,2] Because of this development, they are being used for *in vitro* pharmacological and pathological studies worldwide.[3–5] Particularly in the process of drug discovery, the establishment of high-precision procedures for the assessment of drug efficacy and adverse reactions using human PS cell-derived cardiomyocytes in preclinical studies is expected to improve the efficiency of the drug discovery process and the safety of new drugs, as well as reduce animal experimentation.[6–8]

Parameters that must be measured in *in vitro* drug studies using human PS cell-derived cardiomyocytes can be classified into two general categories: electrophysiological parameters and contractility. Electrophysiological parameters can be assessed by the patch-clamp measurement of membrane potentials and multi-electrode array (MEA) measurement of extracellular field potentials.[9] The assessment of drug's effects on action potential duration of PS cell-derived cardiomyocytes by these methods have been shown to allow the prediction of fatal arrhythmogenic risk more precisely than before.[10,11] Furthermore, a system has recently been developed that combines technologies in tissue engineering and flexible electronics to allow monitoring of extracellular field potentials on dynamically beating cardiac tissues created from human PS cell-derived cardiomyocytes.[12]

The assessment of contractility is expected to be useful, particularly in the development of anticancer agents, because they often have adverse effects on cardiac contractility.[13–15] Contractility of human PS cell-derived cardiomyocytes can be assessed by imaging analysis[16] and impedance assays.[17] These methods measure the micro-movements of cardiomyocytes as the index of contractility, thus offering the advantage of high throughput. In parallel with such

[a] *Department of Modern Mechanical Engineering, Waseda University, 3-4-1 Okubo, Shinjuku-ku, Tokyo 169-8555, Japan. E-mail: umeshin@waseda.jp*
[b] *Thin-Film Device Laboratory & Center for Emergent Matter Science, RIKEN, 2-1, Hirosawa, Wako, Saitama 351-0198, Japan. E-mail: kenjiro.fukuda@riken.jp*
[c] *Institute of Advanced Biomedical Engineering and Science, Tokyo Women's Medical University, 8-1 Kawada-Cho, Shinjuku-Ku, Tokyo 162-8666, Japan*
[d] *Department of Integrative Bioscience and Biomedical Engineering, TWIns, Waseda University, 2-2 Wakamatsu-cho, Shinjuku-ku, Tokyo 162-8480, Japan*
[e] *Electrical and Electronic Engineering and Information Systems, The University of Tokyo, 7-3-1 Hongo, Bunkyo-ku, Tokyo 113-8656, Japan.*
E-mail: someya@ee.t.u-tokyo.ac.jp

† Electronic supplementary information (ESI) available. See DOI: 10.1039/d1lc00411e

techniques at the cellular level, direct measurements of contractile forces or pulsating pressures of dynamically beating cardiac tissues created from human PS cell-derived cardiomyocytes have also been under development using tissue engineering technology and flexible electronics.[18–24]

The simultaneous measurement of electrophysiological parameters and contractility is indispensable for more advanced prediction of drug efficacy and adverse effects on the heart. This is because the organized beating of a heart is achieved by their elaborate coupling throughout the cardiac tissue.[25] A disorder of this coupling causes disorganized beating, such as fatal arrhythmias. Simultaneous measurement enables not only the assessment of drugs' effects on both parameters at once, but also the analysis of new parameters related to excitation–contraction coupling. Therefore, new insights into the effects of drugs on myocardial function can be obtained. There have been a few reports focusing on the importance of such simultaneous measurements in human PS cell-derived cardiomyocytes.[26–29] These methods are a combination of a rigid MEA substrate and image analysis or impedance assay, where the micro-movements of cardiomyocytes and the extracellular field potential are measured simultaneously.

However, simultaneous measurement of electrophysiological parameters and contractile force in dynamically beating cardiac tissues *in vitro* was not sufficiently developed before. An important challenge is that the conventional electrophysiological assessments require a rigid substrate that prevents the direct measurement of contractility at a tissue level. The beating of cardiomyocytes adhered on a rigid substrate is mechanically restrained, limiting the measurements to only under non-physiological conditions. Moreover, it has been reported that immaturity of PS cell-derived cardiomyocytes may depend on a mechanical restraint due to the rigid substrate.[30,31]

Here, we show a novel system that simultaneously measures contractile force and extracellular field potential of dynamically beating cardiac cell sheet-tissues. The cardiac cell sheet-tissue was formed on flexible electronic sheet comprising a 500 nm-thick parylene film and 100 nm-thick gold electrodes. Dynamic beating of the tissue was confirmed. This beating was enough to quantify the contractile force reproducibly. The extracellular field potential on the electrode was measured as well, without artifacts due to the reversible bending (wrinkles) of the flexible electronic sheet caused by the beating. Thus, the system enables the simultaneous measurement of extracellular field potential and contractile force, which gives a useful new approach for evaluating drug effects on cardiac function.

Principle of contractile force and the field potential simultaneous measurement system

A schematic illustration of the developed system and a photograph of the system are shown in Fig. 1a and b. Additionally, the structure of the flexible electronics, a photograph, and the detailed fabrication process are shown in Fig. 1c, d, and S1.† The flexible electronics comprise a parylene-SR film and gold electrodes for extracellular field potential measurements. There is a chuck handle on either end of the flexible electronics: one to be connected to the load cell for contractile force measurements, and the other to be affixed to the culture vessel. The total thicknesses of the fabricated flexible electronics substrates were 500, 1000, and 1500 nm, respectively. The flexible electronics are very thin, only about several tenths of the approximately 20 μm-thick cardiac cell sheet-tissues cultured on the flexible electronics.

Human iPS cell-derived cardiomyocytes were cultured to a confluent state on a 12 mm-square area on each flexible electronics, which was coated with fibronectin to improve cell adhesion. After several days of culture, cardiac cell sheet-tissue that had formed on the flexible electronics pulsated synchronously. A confocal fluorescence microscopic image of cardiac troponin-T in the cardiac cell sheet tissue revealed that striated sarcomeric structures were formed (Fig. 1e). Once peeled off from the supporting glass, the flexible electronics with cardiac cell sheet-tissue was bent with the beating (Movie S1–S3†). Therefore, its flexibility was demonstrated. Live/dead staining showed that detachment of the flexible electronics with cardiac cell sheet tissue from the glass substrate had little effect on cell viability (Fig. S2†).

The chuck handle was affixed to the culture vessel. Pull-out electrodes were then connected to the extracellular field potential measurement system through a printed circuit board (PCB). The other chuck handle was connected to the load cell for contractile force measurements through a connecting rod. The principle of the system to simultaneously measure contractile force and extracellular field potential of cardiac cell sheet-tissues is detailed in Fig. 1f. The end of the flexible electronics connecting to the extracellular field potential measurement system was completely affixed. Therefore, the compressive strain on the flexible electronics generated by the beating cardiac cell sheet-tissue was transmitted to the load cell, thereby making it possible to measure the contractile force.

Characterization of the simultaneous measurement system

Prior to conducting simultaneous measurements of contractile force and extracellular field potential of cardiac cell sheet-tissues, the requisite thickness of the flexible electronics for quantitative measurements of contractile force was examined. Cardiomyocytes were cultured on flexible electronics under the same conditions to thicknesses of 500, 1000, and 1500 nm, respectively. The contractile force of cardiac cell sheet-tissues that formed after 1-week culture was measured and compared. A force of 0.07 mN, 10-fold the standard deviation of noise, was considered the lower limit of quantification of contractile force measurements. The contractile forces are compared in Fig. 2a, and an example of a contractile force waveform comparison is

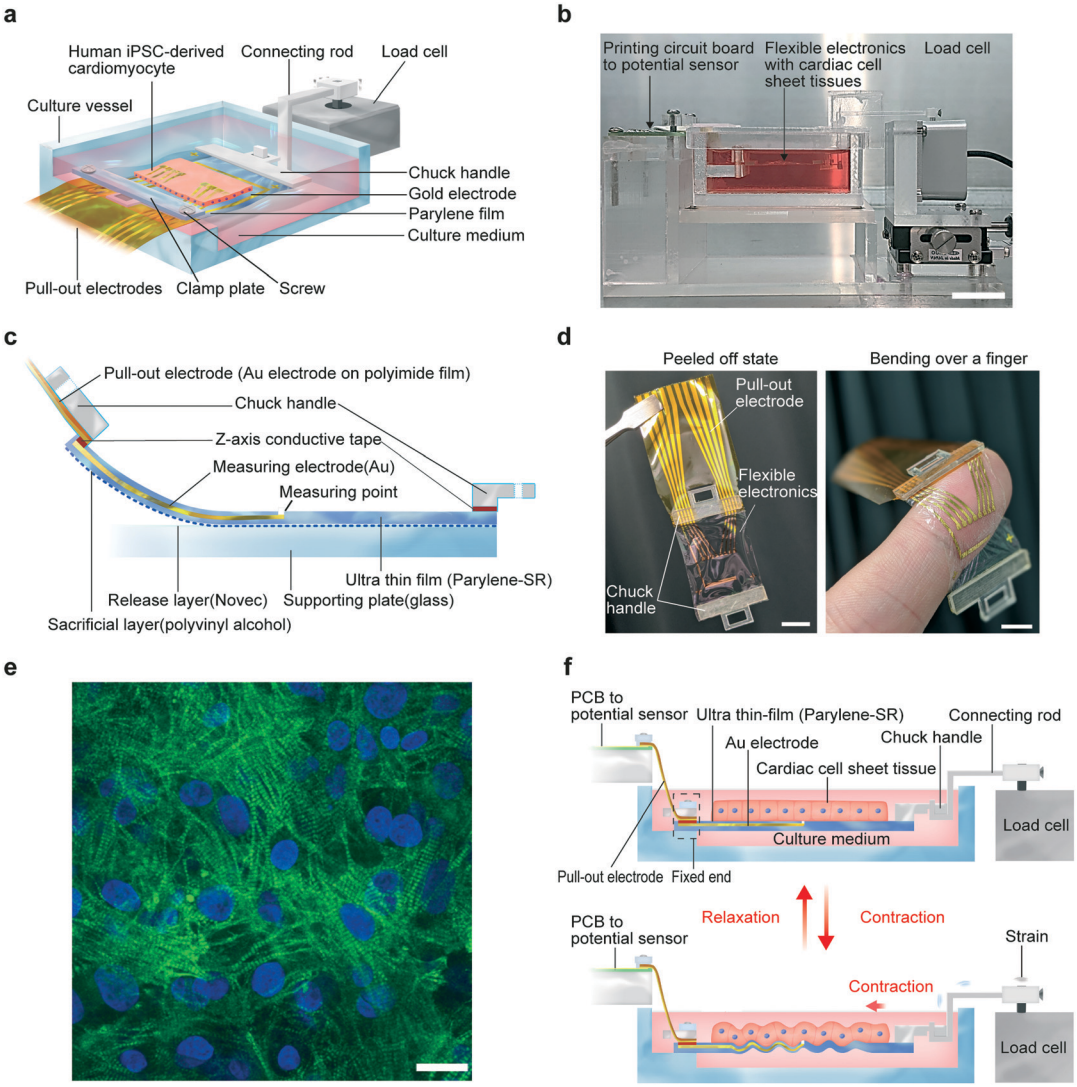

Fig. 1 System for the simultaneous measurement of field potential and contractile force of human iPS-derived cardiomyocytes. (a), Schematic illustration of the simultaneous measurement system. (b), Optical image of the simultaneous measurement system (scale bar, 2 cm). (c), Composition of the flexible electronic sheet for simultaneous measurement. (d), Optical image of the flexible electronic sheet peeled off state (left) and bent over a finger (right) (scale bar, 1 cm). (e), Confocal fluorescence microscopy of cardiac cell sheet tissue. Cardiac troponin-T (green) and nuclei (blue) were stained fluorescently (scale bar, 20 μm) (f), measuring principle of the simultaneous measurement system.

shown in Fig. 2b. The measured contractile force increases as the substrate becomes thinner. This is thought to be due to the fact that thin substrates are easily deflected. Of all the cardiac cell sheet-tissue samples assessed, contractile forces could be quantified when the tissues were cultured on the 500 nm-thick flexible electronics. Thus, it was confirmed that the 500 nm thickness of electronics was sufficiently flexible to quantify the contractile force. Furthermore, it became relatively difficult to handle flexible electronics thinner than 500 nm without damaging them because thin substrates are more easily to break shown by the results of the tensile test (Fig. S3†). Considering the trade-off between thinness and the handling operation, we decided to use 500 nm-thick flexible electronics for all subsequent experiments.

As stated previously, cardiac cell sheet-tissues generate wrinkles on the flexible electronics corresponding to their beating. To investigate whether such wrinkle affects the electrodes' properties, thereby creating artifacts in the extracellular field potential waveform, changes in electrode impedance were measured after subjecting the flexible electronics to a compressive strain of 20% (Fig. 2c). The compressive strain was applied to flexible electronics and wrinkles were generated by placing the flexible electronics on a pre-stretched elastomer and then relaxing the stretched elastomer (Fig. S4†). The red lines in the figure represent the baseline impedance curve, and the blue lines represent the impedance curve after compressive strain. There was no effect of the compressive strain. That is, the results indicate that the dynamic beating of cultured cardiac cell sheet-tissues on the flexible electronics does not affect the extracellular field potential waveforms.

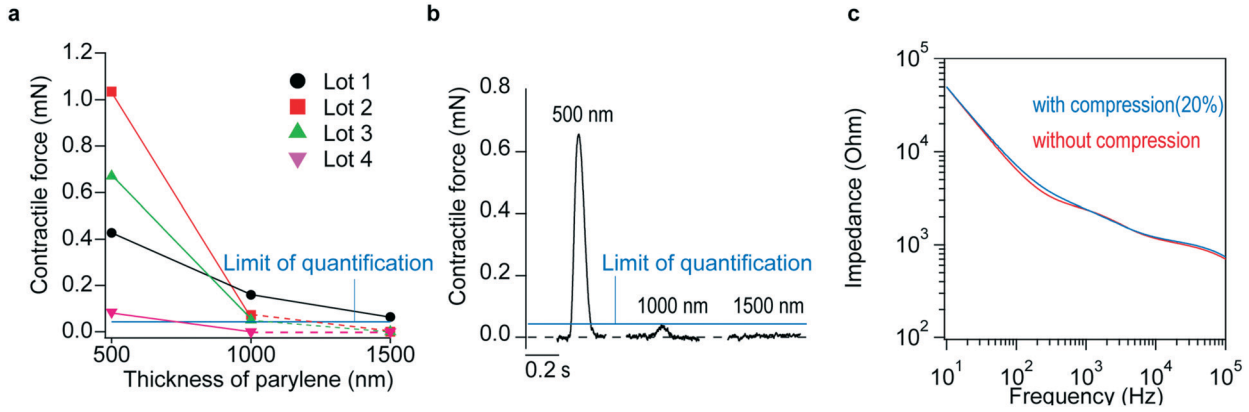

Fig. 2 Characteristics of the simultaneous measurement system. (a), Relationship between the thickness of the flexible electronics and the measured peak contractile force. (b), Comparison of contractile force waveforms by thickness of flexible electronics. The waves are representative waveforms of lot 3. (c), Changes in electrical characteristics before and after applying 20% compressive strain. The impedance curves are means of three flexible electrodes.

Simultaneous measurement of contractile force and extracellular field potential

Contractile forces and extracellular field potentials of human iPS cell-derived cardiac cell sheet-tissues were measured by the developed system (Fig. 3a). The points of the electrodes for measurement were arrayed as shown in Fig. 3b. The results confirmed that the contractile force and extracellular field potentials at 4 different points of the cardiac cell sheet-tissues were successfully measured simultaneously. There was a slight difference in the amplitude and shape of the extracellular field potential waveform depending on the measurement electrode. This variation depends on the expression level of ion channels in the cardiomyocytes above the electrode and the distance between the electrode and the cardiomyocytes. This variation is a general phenomenon and has also been reported in the measurement using MEA.[32] The superimposed waveforms of contractile force and extracellular field potential are shown in Fig. 3c. The waveforms revealed that the force began to rise almost simultaneously with the negative spike in the extracellular field potential waveform due to the Na^+ influx. Subsequently, the force reached its peak. During a relaxation phase, a small positive peak appeared in the field potential wave form due to K^+ efflux. After that, the relaxation phase finally came to an end. In this way, a sequence of events in cardiac electrophysiological activity and mechanical beating was captured. The result demonstrates that this system can be used to analyze in detail the process of excitation–contraction coupling in cardiac cell sheet-tissues. Additionally, millisecond-order time lags between the electrophysiological activities on different electrodes could be detected by superimposing the field potential waveform of each channel (Fig. 3d). This time lags are thought to be due to the propagation of action potentials in the tissue. It is confirmed the expected time and spatial resolution of this system.

Assessment of blebbistatin and adrenaline administration

We demonstrated that the developed system was able to properly assess the effect of blebbistatin (myosin II-specific blocker, 1 μM) and adrenaline[33] (β-receptor agonist, 1 μM) on contractility and the extracellular field potential. We analyzed peak contractile force, beats per minute (BPM), field potential duration (FPD) corrected by Fridericia's formula (FPDcF), contraction time, relaxation time, and force duration 80 (Fig. S5†).

The administration of blebbistatin decreased the contractile force below the limit of quantification. In contrast, the extracellular field potential waveforms showed little change (Fig. 4a and S6†). The results also demonstrate again that the extracellular field potential waveforms are not affected by the compressive strain on the flexible electronics associated with beating. There were no significant changes in BPM and FPDcF with blebbistatin administration (Fig. 4b).

The administration of adrenaline increased the contractile force and BPM, with the contraction waveform becoming sharper (Fig. 4c). The analytical results (Fig. 4d) showed that adrenaline administration significantly increased peak contractile force and BPM and significantly reduced contraction time, relaxation time, and force duration. There was no significant change in FPDcF. The increase in force by administration of adrenaline was relatively smaller than that of human adult myocardium. The difference is likely due to the immaturity of the cardiomyocytes.

Assessment of E-4031 administration

We demonstrated that the developed system was able to assess the effect of E-4031 on FPDcF, which is important for the prediction of fatal arrhythmogenicity. Furthermore, we analyze for the first time the effect of E-4031 on the electro-mechanical window (EMW) in human PS cell-derived cardiac tissues *in vitro*. E-4031 is a human ether-a-go-go related gene

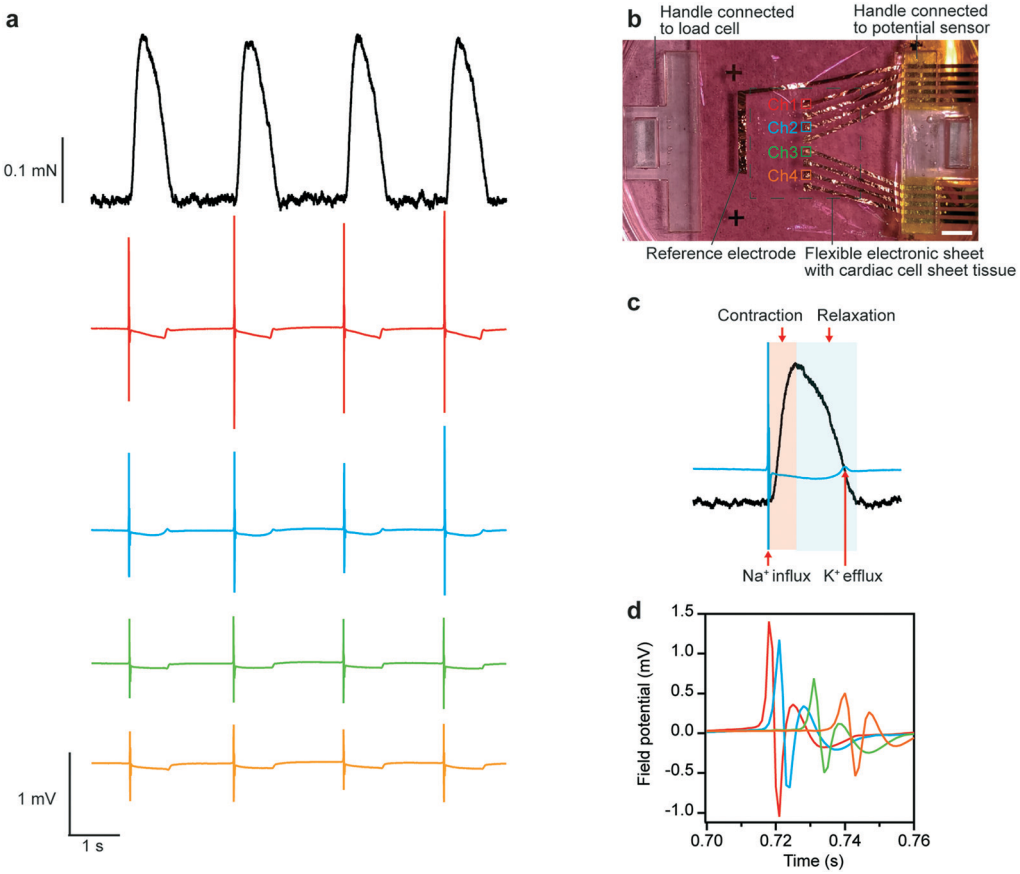

Fig. 3 Simultaneous measurement of contractile force and extracellular field potential. (a), Recorded contractile force and field potential at four points simultaneously. (b), Optical image of cardiomyocytes during measurement and arrangements of measurement points (scale bar, 5 mm). (c), The sequence of excitation–contraction coupling. (d), Expanded view of the field potential at each measuring point.

(hERG) channel blocker, the development of which as a medicine was stopped by its fatal arrhythmogenicity seen in a clinical study.

Fig. 5a shows the representative waveforms of contractile force and field potential before and after the administration of 100 nM E-4031. Fig. 5b shows the representative field potential waveforms before and after the E-4031 administration in which the time scale was corrected by Fridericia's formula. Fig. 5c shows the analytical results for each parameter of contractile force and field potential. The results show that E-4031 administration significantly reduced peak contractile force and significantly prolonged relaxation time and FPDcF. There were no significant changes in BPM, contractile force duration, and contraction time.

EMW is the interval between the end of the T wave on the electrocardiogram and the end of left ventricular pressure *in vivo*.[34] In the presently developed system, the EMW can be analyzed *in vitro* by calculating the temporal difference between the end of the contractile force and the end of repolarization (Fig. 6a). The analytical result showed that the administration of E-4031 exhibited a reducing trend in EMW, with a change in sign from positive to negative (Fig. 6b). We investigated the effect of changing the choice of the extracellular field potential used for EMW evaluation (Table S1, Fig. S7†). The result suggest that the choice of extracellular field potential has little effect on the results of EMW evaluation.

Discussion

In the assessments of blebbistatin and adrenaline administration, all of the analytical results for contractile and electrophysiological parameters were consistent with the action mechanisms of each drug. In the assessment of E-4031 administration, the prolongation of FPDcF by its hERG channel-blocking activity was also clearly confirmed. As unexpected results, a significant decrease of peak contractile force and significant prolongation of relaxation time were obtained (Fig. 5c). The decrease in contractile force is thought to be caused by the stop of spontaneous action potential firing of immature cardiomyocytes when administered high concentration of E-4031.[35]

As for the prolongation of relaxation time, the following mechanisms can be considered. Human iPS cell-derived cardiomyocytes have immature sarcoplasmic reticulum functions. Thus, the contribution of the NCX-mediated extrusion of Ca^{2+} to relaxation is higher than in matured cardiomyocytes.[36] The NCX-mediated extracellular extrusion of Ca^{2+} is dependent on the membrane potential.[37]

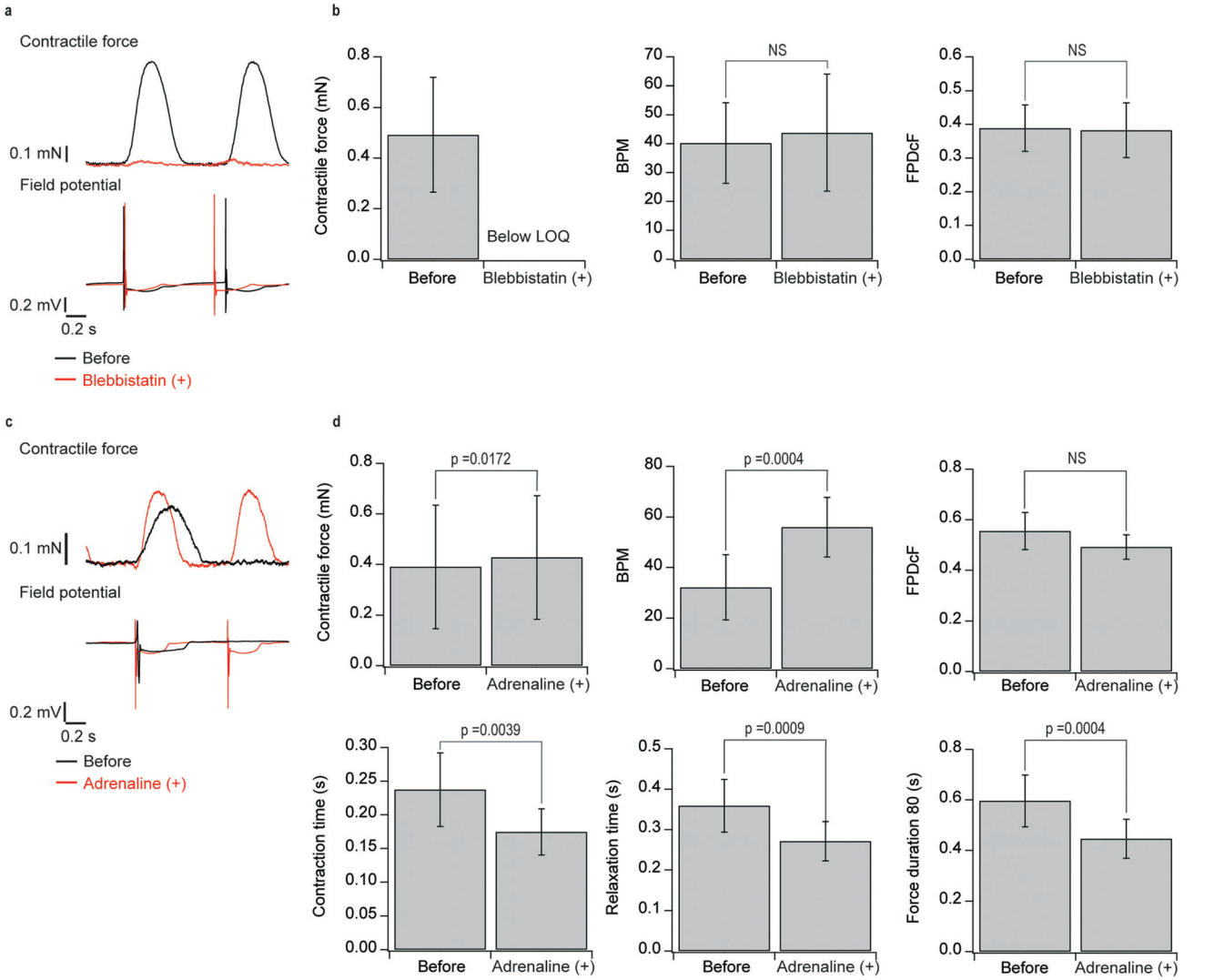

Fig. 4 Assessment of blebbistatin and adrenaline administration. (a), Changes in extracellular field potential and contractile force waveform after administering 1 μM blebbistatin (after 30 minutes). (b), The effect of administering 1 μM blebbistatin on electrophysiological parameters and contractility (contractile force, BPM, FPDcF). Data are presented as means ± SD of 3 cardiac cell sheet-tissues. Data before and after administration are compared with the two-sided paired *t*-test. LOQ = quantitation limit. (c), Changes in extracellular field potential and contractile force waveform after administering 1 μM adrenaline (after 30 minutes). (d), The effect of administering 1 μM adrenaline on electrophysiological parameters and contractility (contractile force, BPM, FPDcF, contraction time, relaxation time, force duration 80). In two of the six samples, analysis of the FPDcF was not possible because the wave of K^+ efflux was below the detectable level. Therefore, the data of FPDcF are presented as means ± SD of 4 cardiac cell sheet-tissues. Other data are presented as means ± SD of 6 cardiac cell sheet-tissues. Data before and after administration are compared with the two-sided paired *t*-test.

Therefore, it is likely that the speed of Ca^{2+} extrusion *via* NCX was decreased by the prolonged action potential duration due to E-4031 administration, resulting in the prolongation of relaxation time. The same phenomenon has also been reported in experimental systems with human iPS cell-derived cardiomyocytes cultured on multielectrode array (MEA) plates.[26] Seen clinically as well, prolongation of the left ventricular isovolumetric relaxation time has been reported in patients with long QT syndrome;[38,39] further research into its relationship with arrhythmogenicity or myocardial maturation is still needed.

The FPD of cardiomyocytes corresponds to the QT interval on the electrocardiogram. Although the prolongation of the QT interval or FPD is presently an important indicator of fatal arrhythmogenicity, it does not completely correspond to the true arrhythmogenicity in the human heart.[6,11] This mismatch makes the screening of drug candidates inefficient in non-clinical studies. Therefore, methods for more precise prediction of arrhythmogenicity are desired. The decrease of EMW from positive to negative is expected to be one of the more precise indicators of fatal arrhythmogenicity,[34,40–43] which has been successfully analyzed by the presently developed system without animal experimentation (Fig. 6b). Although the effectiveness of EMW assessment is still under discussion,[44] the developed system can provide advanced information for establishing the precise prediction of arrhythmogenicity.

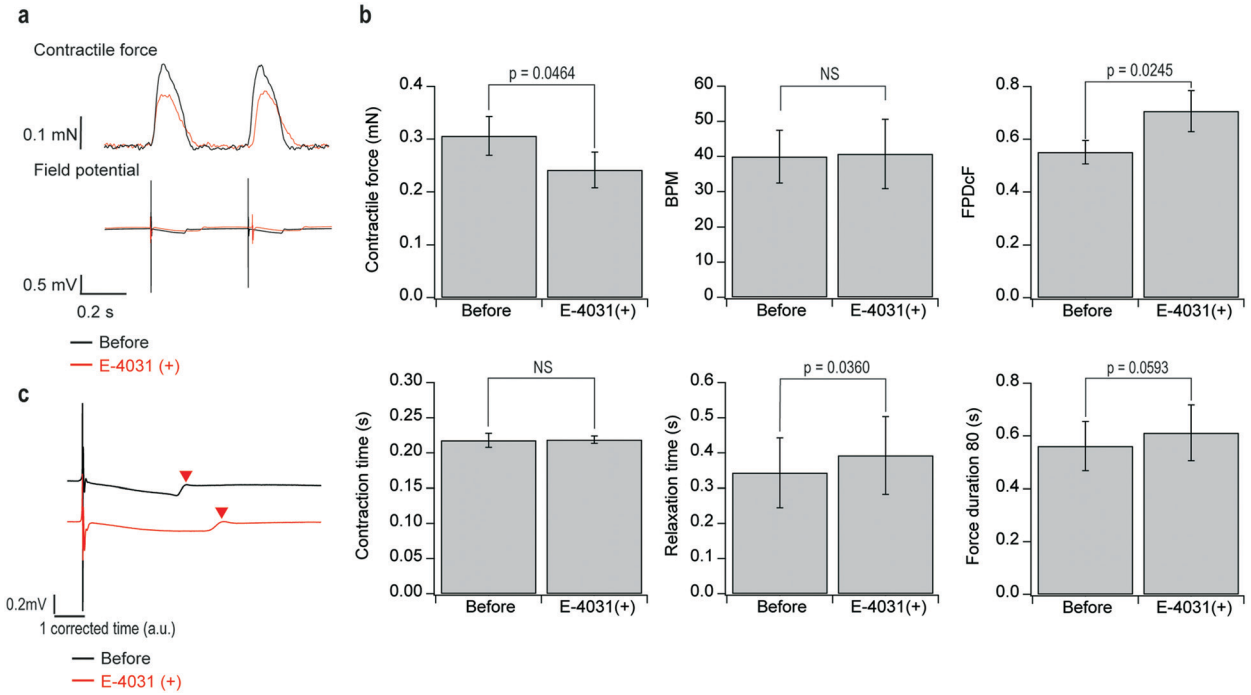

Fig. 5 Assessment of E-4031 administration (a), changes in extracellular field potential and contractile force waveform after administering 100 nM E-4031 (after 5 minutes). (b), Field potential waveform change by administration (red arrow marks show the end point of field potential). Time scale of each wave were corrected by Fridericia's formula. (c), The drug effect of E-4031 on each parameter (contractile force, BPM, FPDcF, contraction time, relaxation time, force duration 80). Data is presented as means ± SD of 3 cardiac cell sheet-tissues. Data between before and after administration is compared with the two-sided paired *t*-test. NS = not significant.

One of the limitations of the newly developed system is the lack of elasticity of the flexible electronics, even though they are flexible enough to be bent. That limitation prevents the stretching and pre-loading of cardiac cell sheet-tissues that actually occur in the natural heart. Potential ways to give elasticity to flexible electronics include the use of a nanomesh or kirigami structure produced by micro-fabrication technology.[12,45] Applying such a technology to this system will make it possible to evaluate drugs under a mechanical environment similar to the natural heart. Additionally, one of the limitations of this system is its low throughput. There are more high-throughput cardio toxicity screening systems which has integrated or rigid readout systems.[9,16,17,26–29] While the throughput of the presently develop system is relatively low, a small number of sophisticated data, corresponding to the natural heart function, can be obtained. To improve the throughput of this system, the difficulty of handling flexible electronics is an

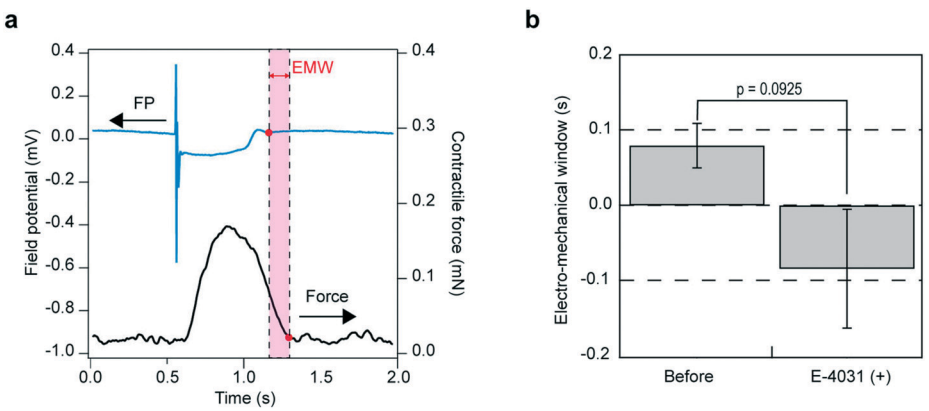

Fig. 6 Evaluation of electro-mechanical window (a), analysis method of electro-mechanical window (EMW). EMWs were calculated as the temporal difference between the end of contractile force and the end of repolarization. (b), The effect of E-4031 on electro-mechanical window. Data is presented as means ± SD of 3 cardiac cell sheet-tissues. Data between baseline and after administration is compared with the two-sided paired *t*-test.

issue that should be solved. The integration of cardiac tissue creation and measurement system is one way to solve this issue.

The measured contractile force varied between samples. We fabricated the 500 nm thick parylene film multiple times and measured the thickness. The thickness of the film was measured by using a stylus profilometer (Dektak XT, BRUKER). The mean thickness of the parylene film was 547 ± 30 nm (mean ± SD of 15 substrates). The coefficient of variation of the contractile force is 0.722 and the coefficient of variation of the thickness of parylene film was 0.055. This result suggests that the variation of the contractile force is not due to the substrate of flexible electronics. Therefore, the influence of variations in quality and maturity of human iPS cell-derived cardiomyocytes is expected to be significant. In the future, further development in technology for producing cardiomyocytes from iPS cells may stabilize data variability.[46]

Furthermore, improving the alignment and synchronization of cardiac cell sheet tissue is also an important issue. The synchronization degree of the cardiac tissue may affect the measured contractile force waves and extracellular field potential waves. When the cardiac cell sheet tissue is synchronized, the contractile force waves will become larger and sharper, and the extracellular field potential waves will become more identical and synchronized. On the other hand, when the cardiac cell sheet tissue is less synchronized, the contractile force waves will become smaller and blunter, and the extracellular potential waves show time lags among the measuring points. Therefore, the non-synchronized cardiac cell sheet tissue is expected to affect the calculation results of parameters related to excitation–contraction couplings, such as EMW. In this study, cardiac cell sheet tissues were created simply by seeding cells at high density. Furthermore, we confirmed that the choice of the extracellular potential wave used for EMW evaluation had little effect (Fig. S7, Table S1†). This result suggests that the cardiac cell sheet tissue created on flexible electronics is sufficiently synchronized for this type of evaluation. Previous studies have reported the improvement of alignment and synchronization of cardiac cell sheet tissue by microfabrication techniques, electrical and mechanical stimulation.[47–50] It is expected that these techniques will be combined in the future to improve the accuracy of the system. These would improve the robustness of the simultaneous measurement system.

Conclusions

In conclusion, the developed system enables detailed analyses of excitation–contraction coupling in human cardiac tissues *in vitro* and is useful for the multiparametric evaluation of new drug candidates for their drug efficacy and adverse reactions, as well as for establishing new parameters for drug evaluations. This system has a wide range of potential applications in the field of cardiac research.

Materials and methods

Materials and fabrication process of the flexible electronic sheet

The details of the fabrication process of the flexible electronics for the simultaneous measurement system of contractile force and extracellular field potential are shown in Fig. S1.† First, fluorinated polymer (1 : 5 mixture of 3M's Novec 1700 and 7100) and 20 wt% PVA aqueous solution (Mw: 500, Wako Pure Chemical Industries) were spin-coated on glass substrate (size: 33 mm × 25 mm, thickness: 1 mm) as a release layer and a sacrificial layer. Then, a 250 nm-thick parylene-SR (dix-SR, KISCO Ltd) layer was coated on the entire surface by chemical vapor deposition using SCS Labcorter. Next, 100 nm-thick Au electrodes were evaporated on the parylene layer. The detailed design of the electrodes is shown in Fig. S8.† After that, pull-out electrodes, which are fabricated by patterning a 3 nm-thick Cr layer and 100 nm-thick Au layer on a 12.5 μm-thick polyimide film (Du Pont-Toray Kapton®), were conducted to an Au electrode on parylene film by anisotropic conductive tape (3M). Then, chuck handles were attached on both sides of the parylene film on glass by anisotropic conductive tape (3M). Next, a 250 nm-thick parylene layer was coated on the entire surface again. Last, the parylene layers on measuring points of extracellular field potential were removed by a reactive etching method.

Preparation of cardiac cell sheet-tissue on flexible electronics

Human iPS cell line 201B7 was purchased from RIKEN (Tsukuba, Japan). Human iPS cells expressing α-myosin heavy chain promoter and Rex-1 promoter-driven drug-resistance genes were cultured on inactivated mouse embryonic fibroblasts (REPROCELL, Yokohama, Japan) as described in a previous study.[51]

Human iPS cell-derived cardiomyocytes were seeded directly onto the flexible electronic sheet surface. Dulbecco's modified eagle medium was added with 10% fetal bovine serum (FBS) and 1% penicillin–streptomycin to be used as a culture medium. The human iPS cell-derived cardiomyocytes were cultured for 7 days on a 100 mm tissue culture dish. Subsequently, 1.5 μg ml^{-1} puromycin (Sigma-Aldrich) was added for cardiomyocyte purification. After 18–24 h, the medium was changed for a culture medium without puromycin and then cultured for a day. Subsequently, the cardiomyocytes were harvested and seeded at 3.0×10^5 cells per cm^2 into a 12 mm × 12 mm silicone frame placed on the flexible electronic sheet, which was coated by 300 μl of 30 μg ml^{-1} fibronectin to improve the attachment of cardiomyocytes. The cell density was controlled to be high enough to create cardiac cell sheet tissues and adhesion area of cardiomyocyte was also controlled by using the silicone frame. The silicone frame was placed in a position to cover the reference electrode. This arrangement prevents cardiomyocytes from adhering to the reference electrode when seeding them. Furthermore, variations of electric

potential waveform are prevented by forming cardiac cell sheet tissues. The cardiomyocytes were cultured in an incubator (37 °C) with 5% CO_2 for 3 days. Then, the flexible electronic sheet with cardiomyocytes was peeled off from supporting glass and moved into culture dish.

Cell culturing took place in Petri dishes, with the chuck handles on the flexible electronics affixed to an acrylic jig, allowing the flexible electronics to maintain their natural length (Fig. S9†). After being transferred to a Petri dish, samples were cultured for at least 4 days in an incubator before they were moved to the system for simultaneous measurement of contractile force and extracellular field potential.

Immunofluorescence staining

The cardiac cell sheet tissue was fixed with 4% paraformaldehyde, permeabilized with 0.2% Tween 20, and blocked with blocking agent (Blocking one-P, Nacalai Tesque). Immunostaining was performed using the following primary antibodies: mouse anti-cardiac troponin T (cTnT), cardiac isoform, mouse-mono (MS-295-P1, clone 13-11, LVC), and the following secondary antibodies: goat anti-Mouse IgG (H + L) secondary antibody; DyLight 488 (NBP1-75146, NOVUS), DAPI (D3571, Invitrogen). Confocal microscopy images were obtained using an Olympus FluoView 1200 laser scanning confocal microscope.

Integration of flexible electronics with cardiac cell sheet tissues into the simultaneous measurement system

Each sample was affixed to the simultaneous measurement system by chuck handles. The chuck handle on the side of the sample with pull-out electrodes was pressed and affixed by an acrylic screw to a built-in anchor in the culture layer, and the chuck handle on the opposite side was hitched on and affixed to a connecting rod attached to the load cell (Fig. S10†). After a sample was set up, 30 ml of a culture medium were added to the culture vessel. Measurements were taken in a globe box under atmospheric conditions with temperature maintained at 37 °C. The culture medium was then changed to Medium 199 Hanks' salts (12350039, Thermo Fisher Scientific) containing 10% fetal bovine serum and penicillin–streptomycin, in which pH changes are different from those under atmospheric conditions. To prevent contamination, the culture layer was covered with a lid. Then, the pull-out electrodes and the extracellular field potential measurement system were connected through a printed circuit board.

The extracellular field potential measurement system comprised a bioelectric amplifier (AB100H; Nihon Kohden, Tokyo, Japan), a BIO coupler (PB101H; Nihon Kohden), and a housing case (JA-100H; Nihon Kohden). The field potentials of the cardiomyocytes were recorded using a 50 Hz notch filter. The load cell for measuring contractile forces (LVS-10GA; Kyowa Electronic Instruments, Tokyo, Japan) was connected to a strain amplifier (DPM-721B; Kyowa Electronic Instruments). Extracellular field potentials and contractile forces amplified by the respective amplifier were recorded on a personal computer *via* an A/D converter (DC-300H, Nihon Kohden). The sampling rate was set to 1 kHz. The analog sensitivity of the extracellular field potential was set to 1000× for the measurement. However, the units displayed as data are before amplification. The value of the contractile force measured by the load cell was calibrated by hanging some weights. Therefore, the contractile force values measured by the developed system are consistent with the actual contractile force generated by the cardiac cell sheet tissue.

Analysis method

Contractile forces and extracellular field potentials were analyzed using Igor Pro (Wavemetric, Lake Oswego, OR, USA). Contractile forces were calculated as the difference between the mean at baseline, when no contraction force was generated, and the value at the peak of the contractile force waveform. With 20% of the recorded contractile force as a threshold, the time from the threshold to the peak contractile force was considered the contraction time, the time from the peak back to the threshold contractile force was considered the relaxation time, and the sum of contraction time and relaxation time was considered force duration 80. Extracellular field potentials were analyzed by calculating the inter-spike interval (ISI) from the spike indicating Na^+ influx and BPMs from the inverse ratio of ISI. Next, extracellular field potential waveforms were differentiated, and the end of the K^+ efflux wave was calculated from the differentiated waveforms. FPDs were determined as the temporal difference between the end of the K^+ efflux wave that was calculated and the peak of the extracellular field potential spike. Moreover, since FPDs are affected by BPM, corrections are required in comparative analyses. The duration after correction using Fridericia's formula

$$\mathrm{FPDcF} = \mathrm{FPD}/(\mathrm{RR\ interval})^{\frac{1}{3}}$$

was expressed as FPDcF.[52] EMWs were calculated as the temporal difference between the end of the contractile force and the end of repolarization. FPD and EMW were evaluated using an extracellular potential waveform, which has clear enough repolarization waveform to analyse.

Drug tests

To conduct the drug tests, a 5.46 mM stock solution of adrenaline (Bosmin Injection; Daiichi Sankyo, Tokyo, Japan) was diluted with physiological saline to a concentration of 1.5 mM, and blebbistatin (FUJIFILM Wako Pure Chemical Corporation) was dissolved with dimethyl sulfoxide to make a blebbistatin solution at a concentration of 1.5 mM. A 20 μl aliquot of the prepared solution was added to 30 ml of the culture medium in the culture vessel to make a final concentration of 1.0 μM. E-4031 (Sigma-Aldrich Co.) was dissolved with physiological saline to make a 15 μM solution, which was added at an appropriate volume depending on the

desired final concentration. The concentration of drug is determined according to previous study.[16,19,29]

Force and electrical characterization of flexible electronic sheets

To screen for substrate thicknesses that would fully allow the assessment of contractile forces of cardiac cell sheet-tissues cultured on the flexible electronics, 500, 1000, and 1500 nm-thick parylene films were produced. Cardiac cell sheet-tissues were cultured on the films for 1 week before contractile force measurements. Contractile forces were compared among samples prepared with cardiomyocytes that were induced to differentiate at the same time.

To assess changes in electrical characteristics as the flexible electronics contracted along with the beating of the cardiac cell sheet-tissue, an LCR meter (IM3533; Hioki) was used to measure changes in impedance after the application of a compressive strain force. A PBS solution was placed on the electrodes of the flexible electronics to measure impedance by the four-point probe method, with the Ag–AgCl electrode as a reference electrode and the Pt electrode as a counter electrode. A compressive strain of 20% was applied by placing the flexible electronics on a silicone rubber sheet that had been stretched by 20% and then allowed to return to its natural length (Fig. S4†).

Author contributions

T. O. and H. O. fabricated the simultaneous measurement system. T. K., D. S., K. F., T. So and S. U. helped in the design of simultaneous measurement system. T. O., H. O., K. M., and T. Sh. fabricated the hiPSC-derived cardiomyocytes. T. O., H. O., K. F., and T. So contributed fabrication of flexible electronics. T. O., H. O., T. K., D. S., and T. Sh. contributed assessment of drugs. Y. K. took confocal fluorescence microscopy images. T. O. performed data analysis of all samples. S. U. supervised the project. T. O. wrote the initial manuscript, which was edited by all authors.

Conflicts of interest

Tatsuya Shimizu and Katsuhisa Matsuura are inventors of the bioreactor system for differentiation culture of pluripotent stem cells, the patents of which are held by Able Co. and Tokyo Women's Medical University.

Acknowledgements

This work was supported by Japan Society for the Promotion of Science (JSPS) KAKENHI (grant number 19J21529, 19H02117, 17H06149) and The Telecommunications Advancement Foundation.

References

1 K. Takahashi, K. Tanabe, M. Ohnuki, M. Narita, T. Ichisaka, K. Tomoda and S. Yamanaka, *Cell*, 2007, **131**, 861–872.
2 J. A. Thomson, J. Itskovitz-eldor, S. S. Shapiro, M. A. Waknitz, J. J. Swiergiel, V. S. Marshall and J. M. Jones, *Adv. Sci.*, 2009, **282**, 1145–1147.
3 M. Bellin, M. C. Marchetto, F. H. Gage and C. L. Mummery, *Nat. Rev. Mol. Cell Biol.*, 2012, **13**, 713–726.
4 N. Sun, N. Sun, M. Yazawa, J. Liu, L. Han, V. Sanchez-freire, O. J. Abilez, E. G. Navarrete, S. Hu, L. Wang, A. Lee, R. E. Dolmetsch, M. J. Butte, E. A. Ashley and M. T. Longaker, *Sci. Transl. Med.*, 2012, **4**, 130ra47.
5 S. M. Wu and K. Hochedlinger, *Nat. Cell Biol.*, 2011, **13**, 497–505.
6 G. Gintant, P. T. Sager and N. Stockbridge, *Nat. Rev. Drug Discovery*, 2016, **15**, 457–471.
7 H. M. Himmel, *J. Pharmacol. Toxicol. Methods*, 2013, **68**, 97–111.
8 C. W. Scott, M. F. Peters and Y. P. Dragan, *Toxicol. Lett.*, 2013, **219**, 49–58.
9 M. E. Spira and A. Hai, *Nat. Nanotechnol.*, 2013, **8**, 83–94.
10 K. Harris, M. Aylott, Y. Cui, J. B. Louttit, N. C. Mcmahon and A. Sridhar, *Toxicol. Sci.*, 2013, **134**, 412–426.
11 H. R. Lu, E. Vlaminckx, A. N. Hermans, J. Rohrbacher, K. Van Ammel, R. Towart and M. Pugsley, *Br. J. Pharmacol.*, 2008, **154**, 1427–1438.
12 S. Lee, D. Sasaki, D. Kim, M. Mori, T. Yokota, H. Lee, S. Park, K. Fukuda, M. Sekino, K. Matsuura, T. Shimizu and T. Someya, *Nat. Nanotechnol.*, 2019, **14**, 156–160.
13 A. Maillet, K. Tan, X. Chai, S. N. Sadananda, A. Mehta, J. Ooi, M. R. Hayden, M. A. Pouladi, S. Ghosh, W. Shim and L. R. Brunham, *Sci. Rep.*, 2016, **6**, 1–13.
14 P. W. Burridge, Y. F. Li, E. Matsa, H. Wu, S. G. Ong, A. Sharma, A. Holmström, A. C. Chang, M. J. Coronado, A. D. Ebert, J. W. Knowles, M. L. Telli, R. M. Witteles, H. M. Blau, D. Bernstein, R. B. Altman and J. C. Wu, *Nat. Med.*, 2016, **22**, 547–556.
15 V. Schwach, R. H. Slaats and R. Passier, *Front. Cardiovasc. Med.*, 2020, **7**, 1–12.
16 T. Hayakawa, T. Kunihiro, S. Dowaki, H. Uno, E. Matsui, M. Uchida, S. Kobayashi, A. Yasuda, T. Shimizu and T. Okano, *Tissue Eng., Part C*, 2012, **18**, 21–32.
17 L. Guo, R. M. C. Abrams, J. E. Babiarz, J. D. Cohen, S. Kameoka, M. J. Sanders, E. Chiao and K. L. Kolaja, *Toxicol. Sci.*, 2011, **123**, 281–289.
18 S. Tsuruyama, K. Matsuura, K. Sakaguchi and T. Shimizu, *Regen. Ther.*, 2019, **11**, 297–305.
19 D. Sasaki, K. Matsuura, H. Seta, Y. Haraguchi, T. Okano and T. Shimizu, *PLoS One*, 2018, **13**, 1–21.
20 J. U. Lind, T. A. Busbee, A. D. Valentine, F. S. Pasqualini, H. Yuan, M. Yadid, S. J. Park, A. Kotikian, A. P. Nesmith, P. H. Campbell, J. J. Vlassak, J. A. Lewis and K. K. Parker, *Nat. Mater.*, 2017, **16**, 303–308.
21 C. P. Jackman, A. L. Carlson and N. Bursac, *Biomaterials*, 2016, **111**, 66–79.
22 M. Tiburcy, J. E. Hudson, P. Balfanz, S. Schlick, T. Meyer, M. L. C. Liao, E. Levent, F. Raad, S. Zeidler, E. Wingender, J. Riegler, M. Wang, J. D. Gold, I. Kehat, E. Wettwer, U. Ravens, P. Dierickx, L. W. Van Laake, M. J. Goumans, S. Khadjeh, K. Toischer, G. Hasenfuss, L. A. Couture, A. Unger, W. A. Linke,

T. Araki, B. Neel, G. Keller, L. Gepstein, J. C. Wu and W. H. Zimmermann, *Circulation*, 2017, **135**, 1832–1847.

23 K. Ronaldson-Bouchard, S. P. Ma, K. Yeager, T. Chen, L. J. Song, D. Sirabella, K. Morikawa, D. Teles, M. Yazawa and G. Vunjak-Novakovic, *Nature*, 2018, **556**, 239–243.

24 Y. Zhao, N. Rafatian, N. T. Feric, B. J. Cox, R. Aschar-Sobbi, E. Y. Wang, P. Aggarwal, B. Zhang, G. Conant, K. Ronaldson-Bouchard, A. Pahnke, S. Protze, J. H. Lee, L. Davenport Huyer, D. Jekic, A. Wickeler, H. E. Naguib, G. M. Keller, G. Vunjak-Novakovic, U. Broeckel, P. H. Backx and M. Radisic, *Cell*, 2019, **176**, 913–927, e18.

25 D. M. Bers, *Nature*, 2002, **415**, 198–205.

26 T. Hayakawa, T. Kunihiro, T. Ando, S. Kobayashi, E. Matsui, H. Yada, Y. Kanda, J. Kurokawa and T. Furukawa, *J. Mol. Cell. Cardiol.*, 2014, **77**, 178–191.

27 K. S. Kulp and E. K. Wheeler, *Lab Chip*, 2017, **17**, 1732–1739.

28 B. J. van Meer, A. Krotenberg, L. Sala, R. P. Davis, T. Eschenhagen, C. Denning, L. G. J. Tertoolen and C. L. Mummery, *Nat. Commun.*, 2019, **10**, 4325.

29 X. Zhang, L. Guo, H. Zeng, S. L. White, M. Furniss, B. Balasubramanian, E. Lis, A. Lagrutta, F. Sannajust, L. L. Zhao, B. Xi, X. Wang, M. Davis and Y. A. Abassi, *J. Pharmacol. Toxicol. Methods*, 2016, **81**, 201–216.

30 M. Wheelwright, Z. Win, J. L. Mikkila, K. Y. Amen, P. W. Alford and J. M. Metzger, *PLoS One*, 2018, **13**, 1–17.

31 A. J. S. Ribeiro, Y. Ang, J. Fu, R. N. Rivas and T. M. A. Mohamed, *Proc. Natl. Acad. Sci. U. S. A.*, 2015, **112**(41), 12705–12710.

32 K. Asakura, S. Hayashi, A. Ojima, T. Taniguchi, N. Miyamoto, C. Nakamori, C. Nagasawa, T. Kitamura, T. Osada, Y. Honda, C. Kasai, H. Ando, Y. Kanda, Y. Sekino and K. Sawada, *J. Pharmacol. Toxicol. Methods*, 2015, **75**, 17–26.

33 G. Callewaert, L. Cleemann and M. Morad, *Proc. Natl. Acad. Sci. U. S. A.*, 2013, **85**, 2009–2013.

34 H. J. Van Der Linde, B. Van Deuren, Y. Somers, B. Loenders and R. Towart, *Br. J. Pharmacol.*, 2010, **161**, 1444–1454.

35 M. Li, Y. Kanda, T. Ashihara, T. Sasano, Y. Nakai, M. Kodama, E. Hayashi, Y. Sekino, T. Furukawa and J. Kurokawa, *J. Pharmacol. Sci.*, 2017, **134**, 75–85.

36 E. Karbassi, A. Fenix, S. Marchiano, N. Muraoka, K. Nakamura, X. Yang and C. E. Murry, *Nat. Rev. Cardiol.*, 2020, **17**, 341–359.

37 M. P. Blaustein, W. J. Lederer and L. Annunziato, *Psychol. Rev.*, 1999, **79**, 763–854.

38 C. Savoye, D. Klug, I. Denjoy, P. V. Ennezat, T. Le Tourneau, P. Guicheney and S. Kacet, *Eur. J. Echocardiogr.*, 2003, **4**, 209–213.

39 S. A. B. Clur, A. S. Vink, S. P. Etheridge, P. G. Robles De Medina, A. Rydberg, M. J. Ackerman, A. A. Wilde, N. A. Blom, D. W. Benson, U. Herberg, M. T. Donofrio and B. F. Cuneo, *Circ.: Arrhythmia Electrophysiol.*, 2018, **11**, 1–13.

40 P. J. Guns, D. M. Johnson, E. Weltens and J. Lissens, *J. Pharmacol. Toxicol. Methods*, 2012, **66**, 125–134.

41 P. J. Guns, D. M. Johnson, J. Van Op Den Bosch, E. Weltens and J. Lissens, *Br. J. Pharmacol.*, 2012, **166**, 689–701.

42 R. M. A. Bekke, K. H. Haugaa, A. Van Den Wijngaard, J. M. Bos, M. J. Ackerman, T. Edvardsen and P. G. A. Volders, *Eur. Heart J.*, 2015, **36**, 179–186.

43 H. M. Vargas, *Br. J. Pharmacol.*, 2010, **161**, 1441–1443.

44 T. R. G. Stams, V. J. A. Bourgonje, H. D. M. Beekman, M. Schoenmakers, R. Van Der Nagel, P. Oosterhoff, J. M. Van Opstal and M. A. Vos, *Br. J. Pharmacol.*, 2014, **171**, 714–722.

45 Y. Morikawa, S. Yamagiwa, H. Sawahata, R. Numano, K. Koida, M. Ishida and T. Kawano, *Adv. Healthcare Mater.*, 2018, **7**, 1–10.

46 K. Miki, K. Deguchi, M. Nakanishi-Koakutsu, A. Lucena-Cacace, S. Kondo, Y. Fujiwara, T. Hatani, M. Sasaki, Y. Naka, C. Okubo, M. Narita, I. Takei, S. C. Napier, T. Sugo, S. Imaichi, T. Monjo, T. Ando, N. Tamura, K. Imahashi, T. Nishimoto and Y. Yoshida, *Nat. Commun.*, 2021, **12**, 3596.

47 A. Agarwal, J. A. Goss, A. Cho, M. L. McCain and K. K. Parker, *Lab Chip*, 2013, **13**, 3599–3608.

48 J. K. Yip, D. Sarkar, A. P. Petersen, J. N. Gipson, J. Tao, S. Kale, M. L. Rexius-Hall, N. Cho, N. N. Khalil, R. Kapadia and M. L. McCain, *Lab Chip*, 2021, **21**, 674–687.

49 Y. H. Huang, C. F. Yang and Y. H. Hsu, *Lab Chip*, 2020, **20**, 3423–3434.

50 R. K. Jayne, M. Ç. Karakan, K. Zhang, N. Pierce, C. Michas, D. J. Bishop, C. S. Chen, K. L. Ekinci and A. E. White, *Lab Chip*, 2021, **21**, 1724–1737.

51 H. Seta, K. Matsuura, H. Sekine, K. Yamazaki and T. Shimizu, *Sci. Rep.*, 2017, **7**, 1–10.

52 S. Luo, K. Michler, P. Johnston and P. W. MacFarlane, *J. Electrocardiol.*, 2004, **37**, 81–90.